

# Origin of magnetic circular dichroism in GaMnAs: giant Zeeman splitting vs. spin dependent density of states

M. Berciu,<sup>1</sup> R. Chakarvorty,<sup>2</sup> Y. Y. Zhou,<sup>2</sup> M. T. Alam,<sup>3</sup> K. Traudt,<sup>2</sup> R. Jakiela,<sup>4</sup>  
A. Barcz,<sup>4</sup> T. Wojtowicz,<sup>4</sup> X. Liu,<sup>2</sup> J. K. Furdyna,<sup>2</sup> and M. Dobrowolska<sup>2,\*</sup>

<sup>1</sup>*Department of Physics and Astronomy, University of British Columbia, Vancouver, B.C., V6T 1Z1, Canada*

<sup>2</sup>*Department of Physics, University of Notre Dame, Notre Dame, IN 46556, USA*

<sup>3</sup>*Department of Electrical Engineering, University of Notre Dame, Notre Dame, IN 46556, USA*

<sup>4</sup>*Institute of Physics, Polish Academy of Sciences, 02-668 Warsaw, Poland*

(Dated: February 25, 2013)

We present a unified interpretation of experimentally observed magnetic circular dichroism (MCD) in the ferromagnetic semiconductor (Ga,Mn)As, based on theoretical arguments, which demonstrates that MCD in this material arises primarily from a difference in the density of spin-up and spin-down states in the valence band brought about by the presence of the Mn impurity band, rather than being primarily due to the Zeeman splitting of electronic states.

Although a multitude of magneto-optical (MO) studies have attempted to elucidate the effect of magnetism occurring in GaMnAs (both in the epilayer and quantum well forms) on its band properties, their results are conflicting [1–12]. So far the interpretation of the MO data in GaMnAs was carried out using a model similar to that used successfully for II-Mn-VI diluted magnetic semiconductors (DMSs), based on the presence of strong interactions between magnetic moments and electronic bands via  $s, p$ - $d$  exchange, that leads to a *giant Zeeman splitting of electronic states* [13]. Various MO experiments on II-VI DMSs yielded a consistent picture of this exchange mechanism [13]. In particular, it was found that the  $p$ - $d$  exchange constant  $\beta$  (now known with relatively high precision) has antiferromagnetic (AFM) character in all II-VI DMSs, due to virtual transitions between the  $p$  and the half-filled  $3d$  orbitals.

The same approach, when used to analyze MO data in GaMnAs, results not only in a wide range of values for  $\beta$  [2, 4, 12] but, more importantly, in conflicting reports about its sign (FM or AFM) [6, 9, 12], raising questions about the exchange process between Mn moments and band carriers. The correct interpretation of this process is of fundamental importance, since it has major consequences for our understanding of the effect of magnetism occurring in any III-Mn-V system on its band properties, and therefore for possible future applications. The most commonly used technique to study MO properties of GaMnAs is magnetic circular dichroism (MCD), which arises from magnetic-field-induced differences in the absorption of right and left circularly-polarized light, and is given by the expression

$$\text{MCD} = \frac{T^+ - T^-}{T^+ + T^-} \propto \frac{(\alpha^- - \alpha^+)d}{2}. \quad (1)$$

Here  $T^+$  and  $T^-$  are transmission intensities for  $\sigma^+$  and  $\sigma^-$  circular polarizations (which connect the spin-down and spin-up holes with the conduction band states, respectively), and  $\alpha^\pm$  are the corresponding absorption coefficients. When the difference between  $\alpha^+$  and  $\alpha^-$  near

the band gap is caused by a Zeeman shift, the polarity of the MCD signal identifies the sign of the  $p$ - $d$  exchange constant. However, the shape and polarity of the MCD spectrum in GaMnAs is observed to depend on growth conditions [2, 7], resulting sometimes in only positive MCD signal, and sometimes in both negative and positive parts. Application of the Zeeman shift model then leads to a FM (positive MCD) or AFM (negative MCD) signs for  $\beta$ , explaining the contradictory claims in the literature.

However, Zeeman shift is not the only mechanism of MCD. It can also arise due to magnetic-field-induced population changes and/or mixing of states (see, for *e.g.*, Ref. 14). In this Letter we present a unified interpretation of experimental MCD data, supported by theoretical arguments, which demonstrates that MCD in GaMnAs arises primarily from a difference in the density of spin-up and spin-down states in the valence band, brought about by the presence of the Mn impurity band, rather than being primarily due to a Zeeman shift.

GaMnAs samples with thickness of  $0.3 \mu\text{m}$  were grown by molecular beam epitaxy (MBE) on (001) GaAs substrates. Samples with Mn concentration  $x \approx 0.01$  were grown on a  $0.4 \mu\text{m}$  thick ZnSe buffer, while samples with  $x = 0.0003$  and  $0.002$  were grown on a  $0.2 \mu\text{m}$  Ga<sub>0.70</sub>Al<sub>0.30</sub>As buffer. Both buffers serve as excellent etch stops, which allowed us to etch away the GaAs substrate in order to eliminate its contribution to optical transmission. The Mn (and Be, when appropriate) concentrations were determined by secondary ion mass spectrometry (SIMS), showing a very uniform Mn distribution throughout the layers. The Curie temperatures for samples exhibiting FM behavior were obtained from SQUID magnetization data. The MCD measurements were performed in the transmission mode using polarization modulation via a photo-elastic modulator.

Figure 1a shows MCD spectra for a Ga<sub>0.984</sub>Mn<sub>0.016</sub>As sample taken in a magnetic field of 5.0 T at temperatures  $T = 1.7, 20, 40$  and  $70$  K, *i.e.* from well below to

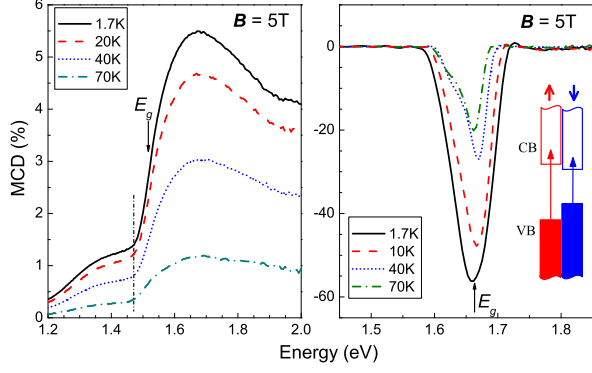


FIG. 1: a) MCD spectra taken at  $B = 5.0$  T and  $T = 1.7, 20, 40$  and  $70$  K on a  $\text{Ga}_{0.984}\text{Mn}_{0.016}\text{As}$  layer grown at  $280^\circ\text{C}$ . The dash-dotted vertical line marks the onset of the sharp rise of MCD. b) MCD spectra taken at  $5.0$  T for similar temperatures on a  $\text{Cd}_{1-x}\text{Mn}_x\text{Te}$  sample with  $x = 0.037$ . The inset shows a schematic illustration of the spin split valence and conduction bands in  $\text{CdMnTe}$ , together with spin conserving transitions allowed for  $\sigma^+$  and  $\sigma^-$  circular polarizations (blue and red lines, respectively).

well above its Curie temperature  $T_C$  of  $26$  K. The MCD spectra show a broad positive signal, which rises sharply in the vicinity of the energy gap, has a peak around  $1.6$ - $1.7$  eV, and extends well beyond the band gap. Similar MCD spectra were observed on FM samples by several other authors [1, 6, 7]. As  $T$  increases, the magnitude of MCD decreases steadily, while the energy at which the sharp rise occurs remains unchanged. This behavior is drastically different from that observed in II-VI DMSs. As an example, Fig. 1b shows the MCD spectra for  $\text{Cd}_{0.963}\text{Mn}_{0.037}\text{Te}$  taken at similar values of  $B$  and  $T$ . Here the MCD shows a negative peak (a consequence of AFM character of the  $p$ - $d$  exchange constant) centered at the energy gap. As  $T$  increases, the spectrum narrows as both its onset and its termination energies shift, reflecting a strong temperature dependence of the  $s$ ,  $p$ - $d$  enhanced giant Zeeman splitting of the band edges [13]. The drastic differences in the shape and temperature dependence of the MCD spectra of these two materials suggests that they likely result from different mechanisms.

The fundamental difference between II-Mn-VI and III-Mn-V systems lies in the fact that the divalent Mn acts as an acceptor in the III-V host. Compared to  $\text{Ga}^{3+}$  ions,  $\text{Mn}^{2+}$  creates a much weaker Coulomb attraction for valence band (VB) electrons. Taking the host's background as reference, this results in an effective repulsive potential near the Mn site, pushing one eigenstate above the VB, thus forming an impurity state near the Mn ion, while the valence band is depleted by one state. Normally this state would be empty (*i.e.*, filled by a hole). However, in a compensated sample this state can be filled by an

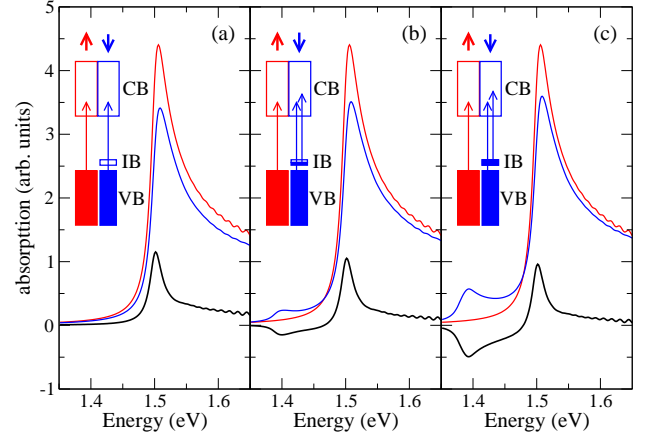


FIG. 2: MCD signal (black line) and  $\alpha^-$ ,  $\alpha^+$  (red, blue lines) calculated for a 1D doped system which is (a) uncompensated, (b) partially compensated, and (c) fully compensated. The corresponding allowed transitions are shown schematically in the insets. The sharp peaks seen at  $E_g$  reflect the 1D density of states (DOS) which diverge at the band-edges.

electron from a donor, such as  $\text{As}_{\text{Ga}}$ . Since  $\text{Mn}^{2+}$  is magnetic, the energy of this state is determined not only by the effective repulsion, but also by the AFM  $p$ - $d$  exchange which contributes a fair amount to the total “binding” energy [15]. This leads to AFM correlations between the spin of  $\text{Mn}^{2+}$  and of the hole (FM correlations with the electron, in compensated samples) occupying the impurity level. Consequently, there is one fewer electron state with spin oriented parallel to the Mn spin left in the valence band.

We will now discuss the MCD spectrum of a sample with a low Mn concentration  $x$ , where the impurity levels have broadened into an impurity band (IB). For that purpose we calculated, using the standard Kubo formula [16], the  $\alpha^+$  and  $\alpha^-$  absorption spectra using a one-dimensional (1D) “toy model”. The VB and CB (conduction band) were modeled by nearest neighbor hopping on two sublattices, with hopping integrals chosen to give reasonable effective masses and an on-site potential on one sublattice chosen to give a gap of  $1.5$  eV.  $\text{Mn}^{2+}$  ions were assumed to be randomly distributed on sites of the VB sublattice. For simplicity, we assumed them to be fully spin polarized by an applied magnetic field, and chose their impurity potential and AFM  $p$ - $d$  exchange with VB electrons so as to give a binding energy of  $0.1$  eV. The results shown in Fig. 2 are for a system with  $N = 500$  sites per sublattice and  $10$  Mn ( $x = 0.02$ ). The oscillatory behavior seen at higher energies is a result of finite-size effects in the density of states. Minimizing this effect requires large  $N$  and is the reason why 3D calculations, which involve full diagonalization of matrices of linear dimension  $\sim N^3$ , are effectively impossible.

Fig. 2a shows  $\alpha^\pm$  absorption spectra and the resulting MCD signal for a sample with an empty IB (no com-

pensation). As sketched in the inset, contributions to  $\alpha^\pm$  come only from VB  $\rightarrow$  CB transitions, both starting at the band gap energy  $E_g = 1.5$  eV. Assuming that the Mn spins are fully polarized by the applied magnetic field, there are  $1 - x$  times fewer spin-down states than spin-up in the VB, and consequently  $\alpha^+$  absorption is weaker than  $\alpha^-$  absorption (blue vs. red lines). This spin dependent difference in the DOS of the VB leads to a positive MCD signal (black line in the figure), which rises sharply at the energy gap. If the system is partially (Fig. 2b) or fully (Fig. 2c) compensated, transitions from IB to CB will also take place. However, since the impurity band states are now occupied by spin-down electrons, these transitions will contribute only to the  $\alpha^+$  absorption. Therefore the difference between the two absorptions due to IB-to-CB transitions will now result in a negative contribution to the MCD signal starting at an energy  $E_g - \Delta_{BE}$  (where  $\Delta_{BE}$  is the binding energy), *i.e.*, about  $\sim 1.4$  eV, and extending into higher energies. Above  $E_g$  the MCD signal will have two competing contributions for compensated samples: a positive contribution arising from the difference in the density of states in the VB (as discussed above), and a negative contribution due to IB-to-CB transitions. The resulting MCD signal will then depend on the degree of compensation, as well as on the matrix elements of the contributing transitions.

As discussed above, we used a simplified 1D model in our calculations. Since the 3D DOS vanishes at the band-edges, one expects the MCD signal to peak at an energy higher than  $E_g$ , where the DOS in the VB is depleted the most by contributions to the IB. For a simple impurity wavefunction  $\langle \vec{r} | I \rangle \sim \exp(-r/a_B)$ , the contribution from VB states of momentum  $k$  is  $p(k) \propto k^2 |\langle \vec{k} | I \rangle|^2 \propto k^2 (k^2 + 1/a_B^2)^{-2}$  ( $k^2$  is due to phase-space volume). Contributions from heavy-hole (hh) states with energy  $\epsilon_h(k) = \hbar^2 k^2 / 2m_h$  are then  $p(\epsilon) = p(k) dk / d\epsilon \sim \sqrt{\epsilon} (2m_h \epsilon / \hbar^2 + 1/a_B^2)^{-2}$ , with a maximum at  $\epsilon_h = \hbar^2 / (6m_h a_B^2)$ . Since optical transitions conserve momentum, the maximum of the MCD signal due to the difference in DOS between the spin-up and spin-down states in the VB should then occur at an energy  $E_{\max} = E_g + \epsilon_h + \epsilon_e$  where  $\epsilon_e = \hbar^2 / (6m^* a_B^2)$ ,  $m^*$  being the CB effective mass. For light holes (lh) one gets a similar formula, but with the hh mass replaced by the lh mass in  $\epsilon_h$ . Using typical values  $a_B \sim 10 \text{ \AA}$ ,  $m_h \sim 0.5m_e$ , and  $m_l \sim m^* \sim 0.07m_e$  gives  $E_{\max} \sim 1.71, 1.86$  eV for hh and lh, respectively. These very rough estimates are consistent with the MCD spectrum shown in Fig. 1a for a sample with very small degree of compensation. The above model explains not only the sign of the MCD signal and the energy range where it peaks, but also the temperature independence of the sharp jump in the positive contribution to MCD, as seen experimentally (see Fig. 1a). According to our model this onset depends only on  $E_g$ , which is temperature independent

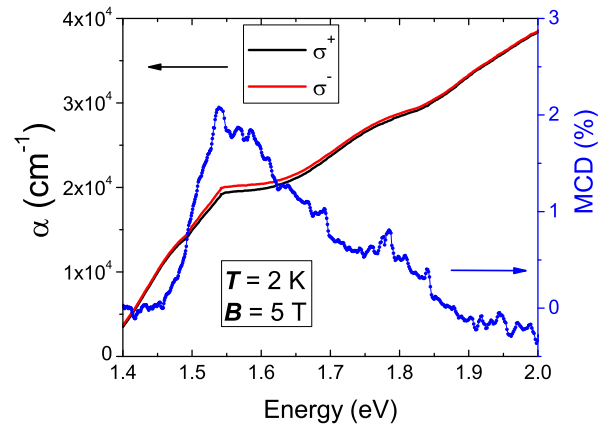


FIG. 3: Absorption spectra of GaMnAs with  $x = 0.0003$  taken at 5 T and  $T = 2$  K for circular polarizations  $\sigma^+$  and  $\sigma^-$ . The corresponding MCD calculated from the  $\sigma^+$  and  $\sigma^-$  absorption curves as  $(\alpha^- - \alpha^+)/2$  is also plotted. The MCD is dominated by a single broad peak centered at 1.565 eV, corresponding to the energy range where  $d\alpha/dE$  is negligible.

in the range studied [17].

The most direct verification of the proposed scenario comes from measurements of  $\alpha^+$  and  $\alpha^-$  at  $B = 5$  T shown in Fig. 3 for a GaMnAs film with  $x = 0.0003$ . The sample was grown at a temperature of  $600^\circ\text{C}$  in order to minimize formation of  $\text{As}_{Ga}$  antisites. An antireflection coating was evaporated onto the sample surface to suppress Fabry-Perot oscillations for photon energies near the band gap. Examination of Fig. 3 indicates that the difference between the  $\alpha^+$  and  $\alpha^-$  curves is mainly caused by a “vertical” rather than “horizontal” shift, suggesting that the difference between the two absorptions is dominated by the difference in the density of states involved in the spin-up and spin-down transitions, rather than by the Zeeman shift of the absorption edges.

We will now compare the predictions of the model with the MCD data shown in Fig. 4a for several GaMnAs films. Samples A, B and D have the same Mn concentration  $x = 0.014$ , but were grown under different conditions, resulting in different levels of compensation: Sample D was grown at  $200^\circ\text{C}$ ; samples A and B were grown at  $250^\circ\text{C}$ ; and sample A was additionally co-doped with Be. As a result, sample D is expected to be highly compensated, while sample A has the lowest degree of compensation. As our model predicts, the below-gap negative contribution to MCD signal is the strongest in sample D, still visible in sample B, but absent in sample A. Above the band gap the positive MCD signal for the highly-compensated Sample D is considerably weaker than for samples A and B. This again is consistent with our model, because the above- $E_g$  MCD signal has two opposite contributions; and since in Sample D the num-

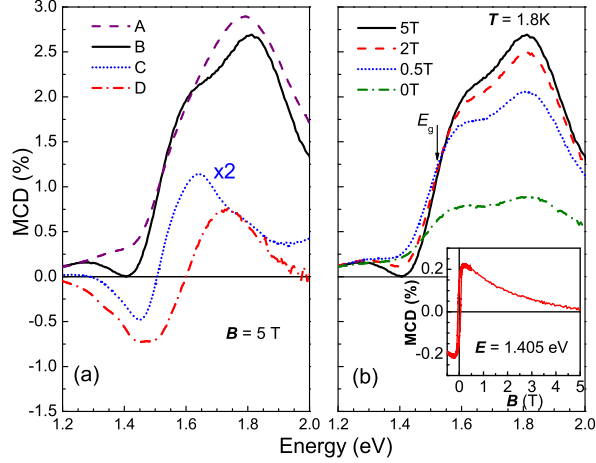


FIG. 4: a) MCD spectra taken at  $T = 1.8$  K and  $B = 5.0$  T for several GaMnAs samples. Samples A, B, and D have  $x = 0.014$ , while sample C has  $x = 0.002$ . For other details, see text. b) MCD spectra taken on sample B at  $T = 1.8$  K and  $B = 0, 0.5, 2$  and  $5$  T. The horizontal line marks  $\text{MCD} = 0$ . Inset: Magnetic field dependence of MCD for sample B observed at  $T = 1.8$  K at photon energy  $1.405$  eV, showing a small but finite hysteresis loop.

ber of spin-down electrons occupying IB is roughly equal to the number of spin-up states depleted from the VB, the resulting signal should be significantly smaller than in samples with lower compensation.

We now consider the shape of the above-gap spectrum. Sample B provides clear evidence for the existence of two MCD peaks above  $E_g$ , at locations consistent with our rough estimates for hh and lh contributions. This identification is further supported by the presence of only one peak (at  $\sim 1.65$  eV) in sample C, grown at  $T_S = 260^\circ\text{C}$  with a much lower Mn concentration  $x = 0.002$ . Since in the single-impurity limit the largest contribution to the impurity state comes from heavy holes [15, 16], we expect to see only the hh peak in the MCD signal for very low  $x$ , as indeed evidenced by sample C. However, as  $x$  increases and the hh states around the optimum energy become exhausted, one expects to see more of the lh states as well as states deeper in the VB being pulled into the IB. This is consistent with the emergence of the second peak (around  $1.85$  eV) in sample B, and the broad unresolved peak at  $\sim 1.8$  eV in sample A.

A final check of our scenario comes from the variation of MCD with changing magnetic field, shown in Fig. 4b for sample B. The FM character of this sample ( $T_C = 16$  K) is evidenced by the presence of MCD signal at zero magnetic field, where, however, we only observe the positive part of MCD produced by interband transitions. The absence of the negative contribution at  $B = 0$  indicates that, even though the sample is FM, the IB states

filled by electrons are not spin-polarized at  $B = 0$ . Only the empty (*i.e.* hole-occupied) states in the IB are spin-polarized, thereby giving rise to a difference in the spin-up and spin-down DOS in the VB, and consequently to a *positive* MCD signal above  $E_g$ . This is fully consistent with the picture proposing that the Mn-Mn interaction in low- $x$  samples is mediated by holes hopping inside an IB [18–21]. Only the Mn ions with high overlap with these holes can be ordered magnetically at  $T_C$ , and in turn polarize the spins of the holes weakly bound to them. The Mn spins with low overlap with the holes, *i.e.*, those with impurity states filled with electrons, remain paramagnetic down to very low temperatures. Since these Mn are not polarized, neither are the electrons filling the states bound to them.

When a magnetic field is applied, however, it polarizes these Mn spins and they in turn polarize their corresponding bound states, which results in a gradual emergence of IB-to-CB transitions, and thus in an onset of a negative contribution to MCD below  $E_g$ . This is precisely the behavior seen experimentally in Fig. 4b. What follows then is that the negative part of MCD must mirror the paramagnetic behavior of the relevant Mn spins. This is verified in the inset in Fig. 4b, which shows that the magnetic field dependence of the MCD signal measured at  $1.4$  eV follows a paramagnetic behavior, even though the hysteresis loop seen in the inset indicates a FM character of the sample as a whole.

In conclusion, this work explains in a unified manner the complex behavior of MCD in GaMnAs that has long been a puzzle in this field. The solution is drastically different from that based on the giant Zeeman shift relevant to II-Mn-VI DMS, and underscores again the importance of the impurity band to our understanding of III-Mn-V DMSs.

This work was supported by NSF Grant DMR 06-03752 as well as NSERC, CIFAR and the Sloan Foundation (M.B.)

\* mdobrowo@nd.edu

- [1] B. Beschoten *et al*, Phys. Rev. Lett. **83**, 3073 (1999).
- [2] T. Hartmann *et al*, Phys. Rev. B **70**, 233201 (2004).
- [3] J. Szczytko *et al*, Solid. State Comm. **99**, 927 (1996).
- [4] J. Szczytko *et al*, Phys. Rev. B **59**, 12935 (1999).
- [5] J. Szczytko *et al*, Phys. Rev. B **64**, 075306 (2001).
- [6] K. Ando *et al*, Phys. Rev. Lett. **100**, 067204 (2008).
- [7] R. Chakarvorty *et al*, App. Phys. Lett. **91**, 171118 (2007).
- [8] W. Heimbrodtt *et al*, Physica E **10**, 175 (2001).
- [9] R. Lang *et al*, Phys. Rev. B **72**, 024430 (2005).
- [10] T. Komori *et al*, Phys. Rev. B **67**, 115203 (2003).
- [11] M. Poggio *et al*, Phys. Rev. B **72**, 235313 (2005).
- [12] R. C. Myers *et al*, Phys. Rev. Lett. **95**, 017204 (2005).
- [13] J. K. Furdyna, J. Appl. Phys. **64**, R29 (1988).
- [14] P. J. Stephens, J. Chem. Phys. **52**, 3489 (1970).
- [15] A. K. Bhattacharjee and C. B. a la Guillaume, Solid State

- Commun. **113**, 17 (2000).
- [16] G. D. Mahan, Many Particle Physics (Plenum, New York, 1981).
  - [17] E. Grilli *et al*, Phys. Rev. B **45**, 1638 (1992).
  - [18] M. Berciu and R. N. Bhatt, Phys. Rev. Lett. **87**, 107203 (2001).
  - [19] A. Kaminski and S. Das Sarma, Phys. Rev. Lett. **88**, 247202 (2002).
  - [20] G. Alvarez, M. Mayr and E. Dagotto, Phys. Rev. Lett. **89**, 277202 (2002).
  - [21] B. L. Shen, *et al*, Phys. Rev. Lett. **99**, 227205 (2007).